Molecular Biology of the Cell
Vol. 14, 2844–2860, July 2003

β-Catenin Regulation during the Cell Cycle: Implications in G2/M and Apoptosis [V]

David Olmeda,* Susanna Castel,† Senén Vilaró,‡ and Amparo Cano*¶

*Instituto de Investigaciones Biomédicas "Alberto Sols," Consejo Superior de Investigaciones Científicas-Universidad Autónoma de Madrid, 28029 Madrid, Spain; †Servicios Científico-Técnicos, Universidad de Barcelona; and ‡Departamento de Biología Celular, Universidad de Barcelona, 08028 Barcelona, Spain

Submitted January 10, 2003; Revised March 11, 2003; Accepted March 11, 2003
Monitoring Editor: Richard Hynes

β-catenin is a multifunctional protein involved in cell-cell adhesion and Wnt signal transduction. β-Catenin signaling has been proposed to act as inducer of cell proliferation in different tumors. However, in some developmental contexts and cell systems β-catenin also acts as a positive modulator of apoptosis. To get additional insights into the role of β-Catenin in the regulation of the cell cycle and apoptosis, we have analyzed the levels and subcellular localization of endogenous β-catenin and its relation with adenomatous polyposis coli (APC) during the cell cycle in S-phase–synchronized epithelial cells. β-Catenin levels increase in S phase, reaching maximum accumulation at late G2/M and then abruptly decreasing as the cells enter into a new G1 phase. In parallel, an increased cytoplasmic and nuclear localization of β-catenin and APC is observed during S and G2 phases. In addition, strong colocalization of APC with centrosomes, but not β-catenin, is detected in M phase. Interestingly, overexpression of a stable form of β-catenin, or inhibition of endogenous β-catenin degradation, in epidermal keratinocyte cells induces a G2 cell cycle arrest and leads to apoptosis. These results support a role for β-catenin in the control of cell cycle and apoptosis at G2/M in normal and transformed epidermal keratinocytes.

INTRODUCTION

β-catenin is a multifunctional protein involved in two essential cellular processes: cell-cell adhesion and Wnt signaling. In intercellular adhesion β-catenin is a component of the cadherin/catenin complexes, which mediate calcium-dependent homophilic interactions (Aberle *et al.,* 1996). As signaling molecule β-catenin is a key effector of the Wnt/Wingless pathway involved in the establishment of the dorso-ventral axis or the segmentation pattern in embryos (Gumbiner, 1995; Willert and Nusse, 1998). The levels of cytoplasmic β-catenin are tightly controlled. In adherent nonstimulated cells, β-catenin is localized at the cell membrane adhesion complexes, whereas the intracellular cytoplasmic levels are kept very low, because of its association with several proteins, APC, GSK-3β, β-TrCP, and axin/conductin, which direct cytoplasmic β-catenin to proteasome-mediated degradation (Rubinfeld *et al.,* 1993, 1996; Munemitsu *et al.,* 1995; Behrens *et al.,* 1998; Liu *et al.,* 1999). Phosphorylation of β-catenin by GSK-3β at specific S/T residues of the N-terminus and a direct interaction with APC is required for productive formation of the destruction complex (Rubinfeld *et al.,* 1996). Activation of the Wnt pathway leads to inhibition of GSK-3β activity, which results in the blockade of the β-catenin phosphorylation and the subsequent stabilization of cytoplasmic β-catenin, which eventually translocates to the cell nucleus. Association of nuclear β-catenin with members of the TCF/Lef family of transcription factors results in the activation of a series of target genes, some of them involved in cell proliferation, such as cyclin D1, c-myc, PPAP-δ and AF17 (He *et al.,* 1998, 1999; Tetsu and McCormick, 1999; Shtutman *et al.,* 1999; Lin *et al.,* 2001). APC mutants unable to downregulate β-catenin as well as mutations of β-catenin abolishing its phosphorylation by GSK-3β lead to stabilization of cytoplasmic β-catenin and transcriptional activation of target genes (Korinek *et al.,* 1997; Morin *et al.,* 1997), supporting a role for β-catenin signaling in

Article published online ahead of print. Mol. Biol. Cell 10.1091/mbc.E03–01–0865. Article and publication date are available at www.molbiolcell.org/cgi/doi/10.1091/mbc.E03–01–0865.

[V] Online version of this article contains video materials for some figures. Online version is available at www.molbiolcell.org.

† Corresponding author. E-mail address: acano@iib.uam.es.

Abbreviations used: APC, adenomatous polyposis coli; GSK-3β, glycogen synthase kinase 3β; MDCK, Madin-Darby canine kidney; MEF, murine embryonic fibroblasts; MTOC, microtubule organizing center; Siah-1, seven in absentia-1 homologous protein.

tumor development (Peifer, 1997). Indeed, activating mutations of β-catenin signaling have been found in different types of tumors (Polakis, 1999).

The positive involvement of β-catenin signaling in cell proliferation has also been supported from a previous report showing that β-catenin controls G1/S transition in MDCK cells (Orford *et al.*, 1999). However, other studies have shown that β-catenin promotes apoptosis in several cell systems, independent of G1/S regulators (Kim *et al.*, 2000) or induces stabilization of p53 and p53/ARF-dependent growth arrest and senescence in mouse embryonic fibroblasts (MEFs) (Damalas *et al.*, 1999, 2001), suggesting a negative role for β-catenin in the control of the cell cycle. A direct implication of β-catenin signaling in apoptosis and cell cycle arrest has been demonstrated in retinal and wing development of *Drosophila* (Ahmed *et al.*, 1998; Johnston and Edgar, 1998). APC is also a multifunctional protein involved in several interactions with the cytoskeleton (for a recent review, see Bienz, 2002). Association of APC with microtubules at the tips of membrane protrusions supported a role in cell migration (Nathke *et al.*, 1996; Nakamura *et al.*, 2001) and a potential modulation of β-catenin turnover (Cui *et al.*, 2002). Association of APC with microtubules at the kinetochores has been recently reported, supporting an additional role for APC in the control of chromosome stability (Fodde *et al.*, 2001; Kaplan *et al.*, 2001). However, the dynamics of β-catenin/APC interaction during the cell cycle and its potential modulation in this key process has not been previously investigated.

We have further investigated the role of β-catenin in the regulation of the cell cycle and apoptosis by performing a detailed study of its levels, subcellular localization and its relation with APC during the cell cycle in several epithelial cell lines. Levels of cytoplasmic β-catenin are dynamically regulated during the cell cycle, increasing during S, accumulating at late G2/M and then abruptly decreasing as the cells enter into a new G1 phase. In parallel, increased cytoplasmic and nuclear localization of β-catenin and APC occurs during S and G2, with a preferential nuclear stain of APC in S and a strong association to centrosome structures in M. Forced accumulation of endogenous β-catenin in epidermal keratinocytes induces a G2 arrest and leads to apoptosis, supporting the need for a tight control of β-catenin levels to ensure the correct progression of cells into the cell cycle.

MATERIALS AND METHODS

Cell Culture and Synchronization

MCA3D (mouse immortalized epidermal keratinocytes) and HaCa4 (mouse squamous cell carcinoma; Navarro *et al.*, 1991) were grown in Ham's F12:DMEM (1:1) medium; PB cells (derived from a mouse skin papilloma; Yuspa *et al.*, 1986); MDCK-II (immortalized canine epithelial kidney cells), and SW480 (human colon carcinoma) in DMEM medium (Life Technologies, Grand Island, NY). All media were supplemented with 10% FBS, 2 mM L-glutamine, and antibiotics, and the cells were grown at 37°C in a humidified 5% CO_2 atmosphere. For G0/G1 synchronization, confluent cells were maintained for 48 h in complete medium followed by 24 h without serum. For S-phase synchronization by double thymidine block, 2×10^5 cells were plated in F-25 flasks and treated with 2.5 mM thymidine (Sigma Chemical Co., St. Louis, MO) in PBS for 24 h. Cells were then washed twice with PBS and twice with complete medium and grown for 9–12 h. Thereafter, the cells were treated with 2.5 mM thymidine in PBS for an additional 18–24 h. Release of the second thymidine block was performed by washing twice with PBS and twice with complete medium. Duplicated cultures were collected after release of the second thymidine block at 1–2-h intervals, as indicated, during a period covering at least a full cell cycle and processed as described below. When indicated, 2 h after release of the second thymidine block, 20 mM LiCl or 20 mM NaCl was added to the culture medium.

Retroviral Transduction and Inducible Cell Transfections

High-titer retrovirus of control pBABE and pBABE-β-catenin(S33Y), containing the HA-epitope tagged β-catenin (S33Y; kindly provided by A. Been Ze'ev, Weizmann Institute, Rehovot, Israel), were obtained by infection of HEK293T cells in the presence of helper virus as described (Damalas *et al.*, 2001). For retroviral transduction PB cells were plated at a density of 2×10^5 cells per 6-cm dish and infected 24 h later with filtered supernatants in the presence of polybrene (8 μg/ml; Sigma Chemical Co.). Fresh supernatants were added three times at 4-h intervals. As control of the infection efficiency, cells were infected with the pBABE-EGFP construction. In three different experiments the efficiency obtained was near 100%.

To generate inducible β-catenin expression, the full human mutant β-catenin(S33Y) cDNA was restriction excised from the plasmid pQE32 (provided by A. Been Ze'ev) and fused to EGFP by cloning into the pEGFP-C1 vector (Clontech, Palo Alto, CA). EGFP-β-catenin(S33Y) was thereafter introduced into the pIND-ecdysone–inducible expression vector (Invitrogen, San Diego, CA) by using appropriate restriction enzymes. After subcloning, all constructions were sequenced and found to be in frame. For transfections, MCA3D cells were plated at 30% confluence in P-60 plates and grown for 24 h in complete medium. They were then transfected with 1.5 μg of pVgRXR (Invitrogen) and pIND-EGFP-β-catenin(S33Y) plasmids, using Lipofectamine Plus transfection system (Life Technologies), following the manufacturer's instructions. When indicated, induction of EGFP-β-catenin(S33Y) expression was performed by adding 1 μM muristerone A (Invitrogen) to the medium.

Flow Cytometry Analysis

Cells growing in F-25 flasks were collected at the indicated time points, trypsinized and centrifuged at 1000 rpm for 10 min, resuspended and washed twice in PBS, and finally fixed in 50% ethanol overnight in suspension. Cells were then centrifuged at 1000 rpm, washed twice in PBS, and resuspended in 1.1% sodium citrate in PBS. Cells were incubated with 200 μg/ml RNAse (Roche Diagnostic, Mannheim, Germany) for 20 min at room temperature and 100 μg/ml propidium iodide was added. The cells were analyzed with a FACScan equipment (Becton-Dickinson, Palo Alto, CA).

Cell Extracts, Immunoprecipitation, and Western Blot Analysis

Soluble and insoluble cell extracts of the different cell lines were obtained as previously described (Lozano and Cano, 1998). Briefly, cells were lysed in 1 ml of NT buffer (5 mM $MgCl_2$, 5 mM $CaCl_2$, 100 mM NaCl, 1% NP-40, 1% Triton X-100, 50 mM Tris-HCl, pH 7.4) in the presence of protease inhibitors, scraped, and centrifuged. The soluble fractions were adjusted to 1× Laemmli buffer, boiled for 4 min, and stored at −20°C. Insoluble fractions were resuspended in 1 ml of 1× Laemmli buffer, passed through a loose needle 10 times and through a tight needle another 10 times, boiled for 4 min, and stored at −20°C. Whole cell extracts were obtained from cells grown in the different conditions using RIPA buffer (50 mM Tris-HCl, pH 7.5, 150 mM NaCl, 1% NP-40, 0.5% deoxycholate, 0.1% SDS). Nuclear extracts were obtained by hypotonic cell lysis (1.5 mM $MgCl_2$,

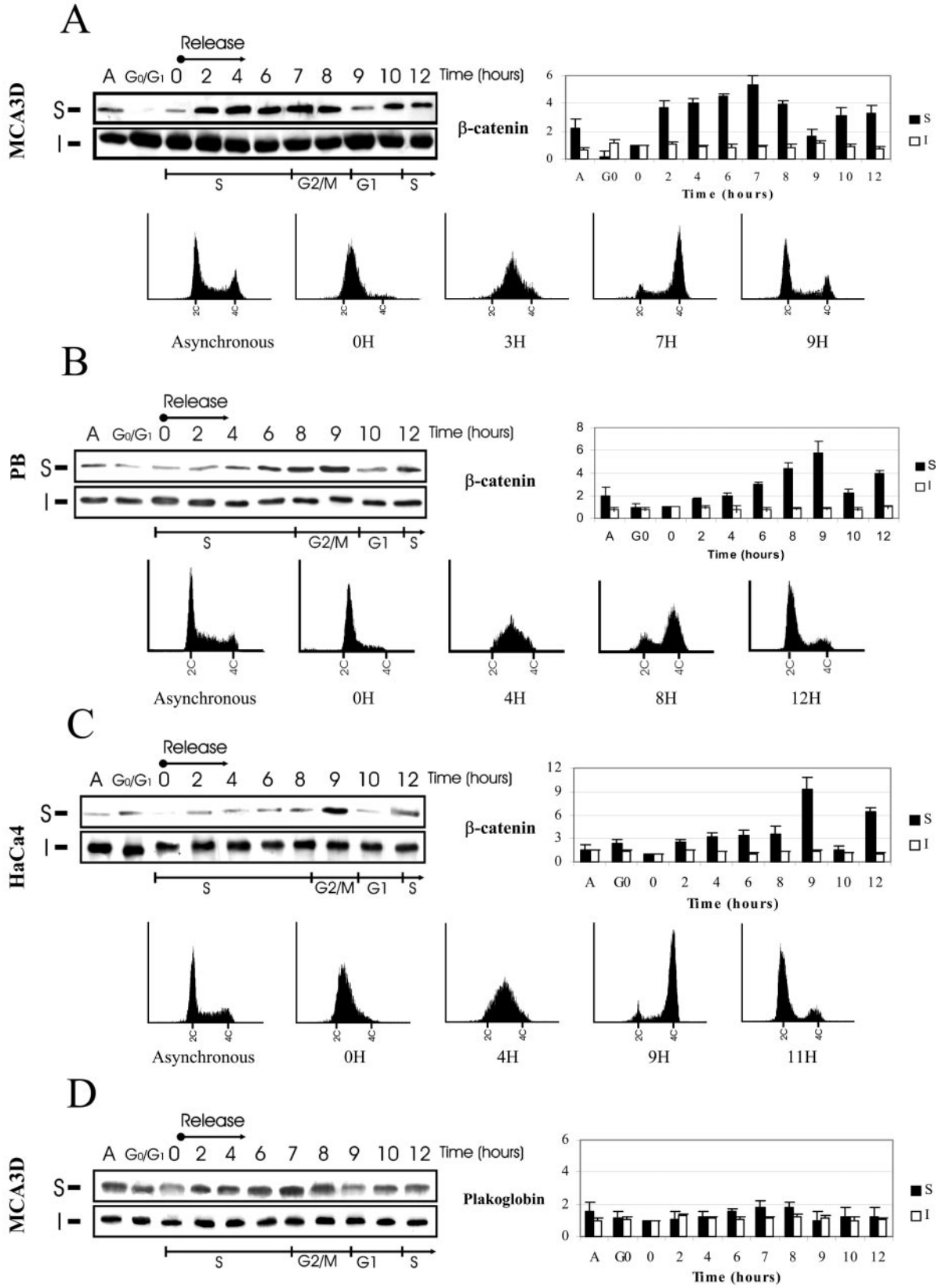
A
Release
A G0/G1 0 2 4 6 7 8 9 10 12 Time (hours)
MCA3D
S
I
β-catenin
S G2/M G1 S
A G0 0 2 4 6 7 8 9 10 12
Time (hours)
S
I
Asynchronous 0H 3H 7H 9H
B
Release
A G0/G1 0 2 4 6 8 9 10 12 Time (hours)
PB
β-catenin
A G0 0 2 4 6 8 9 10 12
Time (hours)
Asynchronous 0H 4H 8H 12H
C
Release
A G0/G1 0 2 4 6 8 9 10 12 Time (hours)
HaCa4
β-catenin
A G0 0 2 4 6 8 9 10 12
Time (hours)
Asynchronous 0H 4H 9H 11H
D
Release
A G0/G1 0 2 4 6 7 8 9 10 12 Time (hours)
MCA3D
Plakoglobin
A G0 0 2 4 6 7 8 9 10 12
Time (hours)

Figure 1.

10 mM KCl, 10 mM HEPES, pH 7.9), isolation of the nuclear fraction and solubilization in saline buffer (420 mM NaCl, 1.5 mM $MgCl_2$, 0.2 mM EDTA, 25% glycerol, 20 mM HEPES, pH 7.9). Immunoprecipitation of soluble fractions (600 μg) with 1.5 μg of anti-APC (N-15, Santa Cruz Biotechnology, Santa Cruz, CA), rat monoclonal anti–E-cadherin (ECCD-2; a gift of M. Takeichi, Kyoto University, Kyoto, Japan), or mouse monoclonal anti–β-catenin antibodies (Transduction Laboratories, Lexington, KY) was carried out as previously described (Espada *et al.*, 1999). For Western blot analysis, equal amounts of total protein (20 μg for nuclear extracts, 30 μg for soluble extracts, and the equivalent volume of the corresponding insoluble fractions, and 30 μg and whole-cell extracts) or immunoprecipitates from each sample were loaded on 7.5, 10, or 12% SDS-PAGE gels. After resolution, the gels were transferred onto Immobilon-P membranes (Millipore Co., Billerica, MA), blocked, and incubated with the appropriate antibodies as described (Lozano and Cano, 1998; Espada *et al.*, 1999). The primary antibodies used included the following: mouse monoclonal anti–β-catenin (1:100) and antiplakoglobin (1:200; Transduction Laboratories), mouse monoclonal anti–α-tubulin (1:1000; Sigma Chemical Co.), and anti-HA (1:2000; Babco, Richmond, CA), rat monoclonal anti–E-cadherin (ECCD-2; 1:200), and rabbit polyclonal anti-APC (N-15; 1:100; Santa Cruz Biotechnology), anti–Siah-1 (1:100) and anti-PARP (1:500; Santa Cruz Biotechnology).

Confocal Immunofluorescence

Cells grown on glass coverslips were washed three times with PBS and fixed either in 4% paraformaldehyde for 10 min at room temperature or 100% methanol (precooled at −20°C) for 4 min and washed in PBS (3×, for 5 min). When indicated, fixed cells were permeabilized with 0.05% NP-40 in PBS for 5 min at room temperature. Slides were incubated with the indicated primary antibodies at optimal dilution for 1 h, washed in PBS (2×, 5 min), and incubated with the appropriate secondary antibody coupled to Alexa 488, FITC, or TRITC for 45 min. TOTO-3 (Molecular Probes, Eugene, OR) or DAPI (Sigma Chemical Co) was used for DNA stain. In the case of TOTO-3, cells were pretreated with RNAse (Roche Diagnostic). Confocal images were obtained with a Leica TCS SPII Spectral microscope and 63×/1.3 NA oil objective. Primary antibodies included the following: mouse monoclonal anti–β-catenin (1:100; Transduction Laboratories), anti-HA (1:1000; Babco), anti–α-tubulin (1:1000) and anti–γ-tubulin (1:500; Sigma Chemical Co), and rabbit polyclonal anti-APC (N-15; 1:100; Santa Cruz Biotechnology), and anti-cyclin B1 (1:100; a gift of C. Calés, Instituto de Investigaciones Biomédicas, Madrid, Spain).

Figure 1 (facing page). Dynamic changes in β-catenin levels during the cell cycle. MCA3D (A and D), PB (B), and HaCa4 (C) cells were synchronized at early S phase by double thymidine block or at G0/G1 by high confluence and serum starvation. After release of the block (time 0 h), soluble and insoluble extracts from indicated time points were obtained. (A) Asynchronous cell populations. The DNA content for each time point was determined by FACS analysis. (A–C) Top left panels: Western blot analysis of β-catenin levels in soluble (S) and insoluble (I) fractions of the indicated cell lines. Densitometric analyses of the levels detected in both fractions are shown at the top right panels (■, soluble; □, insoluble fractions), normalized to the values detected at time point 0 h. Results show the average of three independent experiments ± SD. Flow cytometry analyses of synchronized MCA3D, PB, and HaCa4 cells are shown at the bottom of each panel. (D) Left: Western blot analysis of plakoglobin levels in soluble and insoluble fractions obtained at the indicated time points from synchronized MCA3D cells. Densitometric analysis of the levels detected in both fractions is shown at the right panel (■, soluble; □, insoluble fractions), normalized to the values detected at time point 0 h.

Time-Lapse Video Recording

Time-lapse video recordings were obtained on cells grown in the different experimental conditions in an Axiovert microscope (Zeiss, Thornwood, NY) coupled with a CO_2 and temperature-maintenance system, a CCD camera, and a time-lapse recording system. Confocal time-lapse recording was obtained with a Leica TCS SPII microscope. Digital effects and QuickTime conversion were performed using the Adobe Premiere 6.0 video editing software (San Jose, CA). The specific experimental conditions are indicated in the legends of the corresponding figures.

RESULTS

Dynamic Changes of β-Catenin Levels during the Cell Cycle

To get insights into the regulation of β-catenin through the cell cycle, normal and transformed epithelial cell lines of different origins (mouse epidermal keratinocytes MCA3D, PB and HaCa4, canine kidney MDCK, and SW480 cells) were used. Cells were synchronized at early S phase by double thymidine block and, after release of the block, were allowed to progress through the cell cycle and collected at different time points covering a full cell cycle. The degree of synchronization was confirmed by flow cytometry analysis (Figure 1, A–C, lower panels) and videolapse recording (our unpublished results). β-catenin levels of soluble and insoluble detergent fractions were analyzed by Western blot. As controls, cells synchronized at G0/G1 by high confluence and serum deprivation and asynchronous cell populations were included. In synchronized immortalized MCA3D cells, the soluble levels of β-catenin raised steadily from early S to G2/M up to a 5- to 6-fold increase over the basal levels detected at early S phase (Figure 1A). Analysis of synchronized PB and HaCa4 cells (derived from a papilloma and a squamous cell carcinoma, respectively) showed a similar behavior: a steady increase of soluble β-catenin levels during S phase and maximum accumulation at G2/M of 5- to 6-fold for PB and 9- to 10-fold for HaCa4 cells (Figure 1, B and C). The soluble β-catenin levels in the different cell lines quickly decreased after the cells had divided, reaching the basal levels once the cells are back at early G1, and then started to increase again by late G1 and early S phases (Figure 1, A–C). Soluble β-catenin levels in synchronized MDCK cells showed a similar behavior with a maximum increase of about eightfold at G2/M phase (supplemental Figure 1A). Insoluble β-catenin levels, which are normally considered to be strongly associated to the cytoskeleton, remained constant throughout the cell cycle in all analyzed cell lines (Figure 1, A–C). In contrast with these results, analysis of the soluble levels of plakoglobin in MCA3D and the other cell lines, showed only slight variations (about twofold) during the cell cycle, and no changes were detected in the insoluble fraction (Figure 1D, supplemental Figure 1B), indicating a differential regulation of both catenins during the cell cycle.

The detergent soluble fraction is known to contain cadherin/catenin complexes (Aberle *et al.*, 1996; Lozano and Cano, 1998). To analyze the distribution of β-catenin associated to E-cadherin during the cell cycle, immunoprecipitation analyses of soluble fractions were performed. As shown for MCA3D cells, the levels of β-catenin bound to E-cadherin remained unchanged in the different phases of the cell cycle

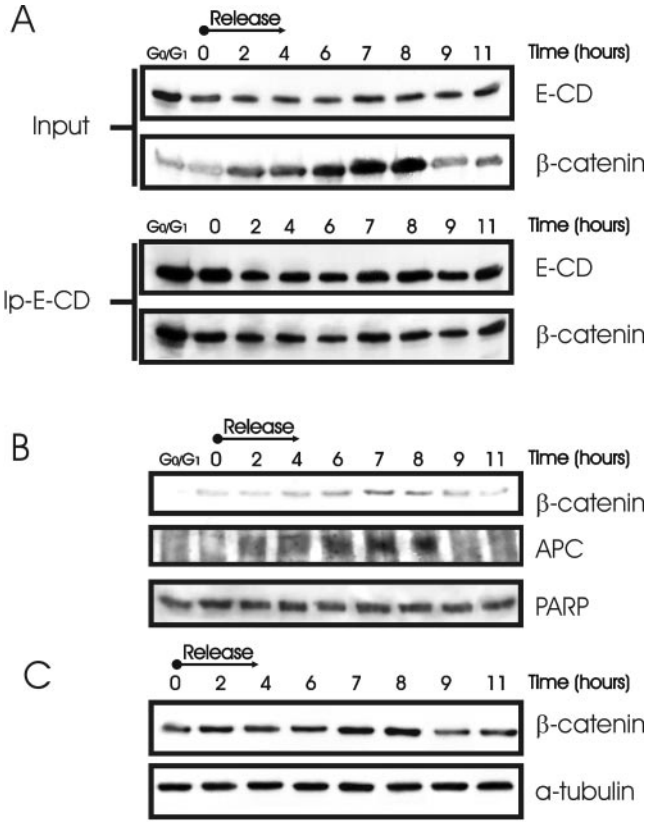

Figure 2. β-catenin nonassociated to E-cadherin accumulates at the cytoplasm and nucleus at S/G2. MCA3D cells were synchronized as described in Figure 1. (A) Top: Levels of E-cadherin (E-CD) and β-catenin in the soluble fractions. Bottom: Coimmunoprecipitation analysis of E-cadherin and β-catenin at the indicated time points. Levels of coimmunoprecipitated E-cadherin (E-CD) and β-catenin were analyzed by Western blot. (B) Western blot analysis of β-catenin (top panel) and APC levels (middle panel) in nuclear extracts of synchronized MCA3D cells. PARP antigen was analyzed as a loading control (bottom panel). (C) Analysis of β-catenin levels during the cell cycle in whole cell extracts. As a loading control, Western blot analysis of α-tubulin was included (bottom panel).

(Figure 2A). These results, together with the fact that HaCa4 cells are deficient in E-cadherin (Navarro *et al.*, 1991) strongly support a neat increase in cytoplasmic β-catenin nonassociated to E-cadherin during S and G2/M phases in epidermal keratinocytes. In addition, analyses of nuclear extracts of MCA3D cells showed a similar increase during S and accumulation at G2/M of nuclear β-catenin and APC levels (Figure 2B). A more slightly increase of β-catenin levels was detected in whole cell extracts (Figure 2C), in agreement with the very high levels of insoluble β-catenin detected in MCA3D cells at all phases of the cell cycle (see Figure 1A).

β-Catenin and APC Accumulate in the Cytoplasm and Nucleus during the Cell Cycle

Accumulation of β-catenin in the cytoplasm normally leads to its translocation to the nucleus. To analyze whether this event is regulated during the cell cycle, subcellular localization of β-catenin at different stages of the cell cycle was determined by confocal immunofluorescence in MCA3D and HaCa4 cells synchronized by double thymidine block. The results obtained with HaCa4 cells are shown in Figure 3. In confluent cells synchronized at G0/G1, β-catenin was mainly detected at the cell-cell contacts and no apparent cytoplasmic staining was observed (Figure 3, G0/G1). Once the cells have entered into S phase, β-catenin started to accumulate in the cytoplasm and nucleus but also remained localized at the cell-cell contacts (Figure 3, early S). By the middle of S phase, a homogenous cytoplasmic and nuclear stain of β-catenin was observed as well as a strong cell-cell contact localization. At late S/G2 phase, β-catenin exhibited the highest cytoplasmic and nuclear stain, maintaining an apparent equal distribution between both cellular compartments (Figure 3, late S/G2), although β-catenin was also present at cell-cell contacts at this stage (the apparent lower intensity at membrane contacts is due to the plane of the confocal image showed in that panel). Once the cells have divided and enter into a new G1 phase, β-catenin was lost from the cytoplasm and nucleus and showed a strong cell-cell contact pattern (Figure 3, G1).

A similar pattern of β-catenin localization during the cell cycle was observed in MCA3D cells (see Figure 6). The changes in β-catenin localization during the cell cycle in epidermal keratinocytes cannot be attributed to differences in cell density, as can be clearly observed from the analyses of MCA3D and HaCa4 cells shown in Figure 6 (control panels), in which cells with equivalent cell densities in S and G2/M phases were analyzed. These results indicate that cytoplasmic accumulation and nuclear translocation of β-catenin is modulated during the cell cycle.

The subcellular localization of APC was analyzed in parallel to β-catenin in synchronized HaCa4 and MCA3D cells. As shown in Figure 3, in HaCa4 cells arrested at G0/G1, APC showed a rather faint stain with some perinuclear granular pattern and no significant colocalization with β-catenin (Figure 3, G0/G1). At early S phase, APC started to accumulate in the cytoplasm and nucleus showing a perinuclear pattern (Figure 3, early S). By the middle of S, an intense nuclear accumulation of APC was detected with an apparent nucleolar exclusion pattern (Figure 3, middle S), in contrast to the more homogeneous distribution between the nucleus and cytoplasm displayed by β-catenin at this stage. At late S/G2 an intense APC nuclear stain was detected with a clear accumulation at one or two bright spots near the nucleus suggestive of centrosome structures. No significant accumulation of β-catenin was detected at these structures (Figure 3, late S/G2, compare β-catenin and APC panels). Once the cells enter into a new G1 phase, APC displayed again a cytoplasmic/perinuclear staining pattern with no significant nuclear accumulation. Localization of APC in some filopodia-like membrane protrusions could also be observed at G1, in agreement with previous reports in asynchronous cell populations (Reinacher-Schick and Gumbiner, 2001). A similar pattern for APC distribution during the cell cycle was observed in synchronized MCA3D cells (our unpublished results).

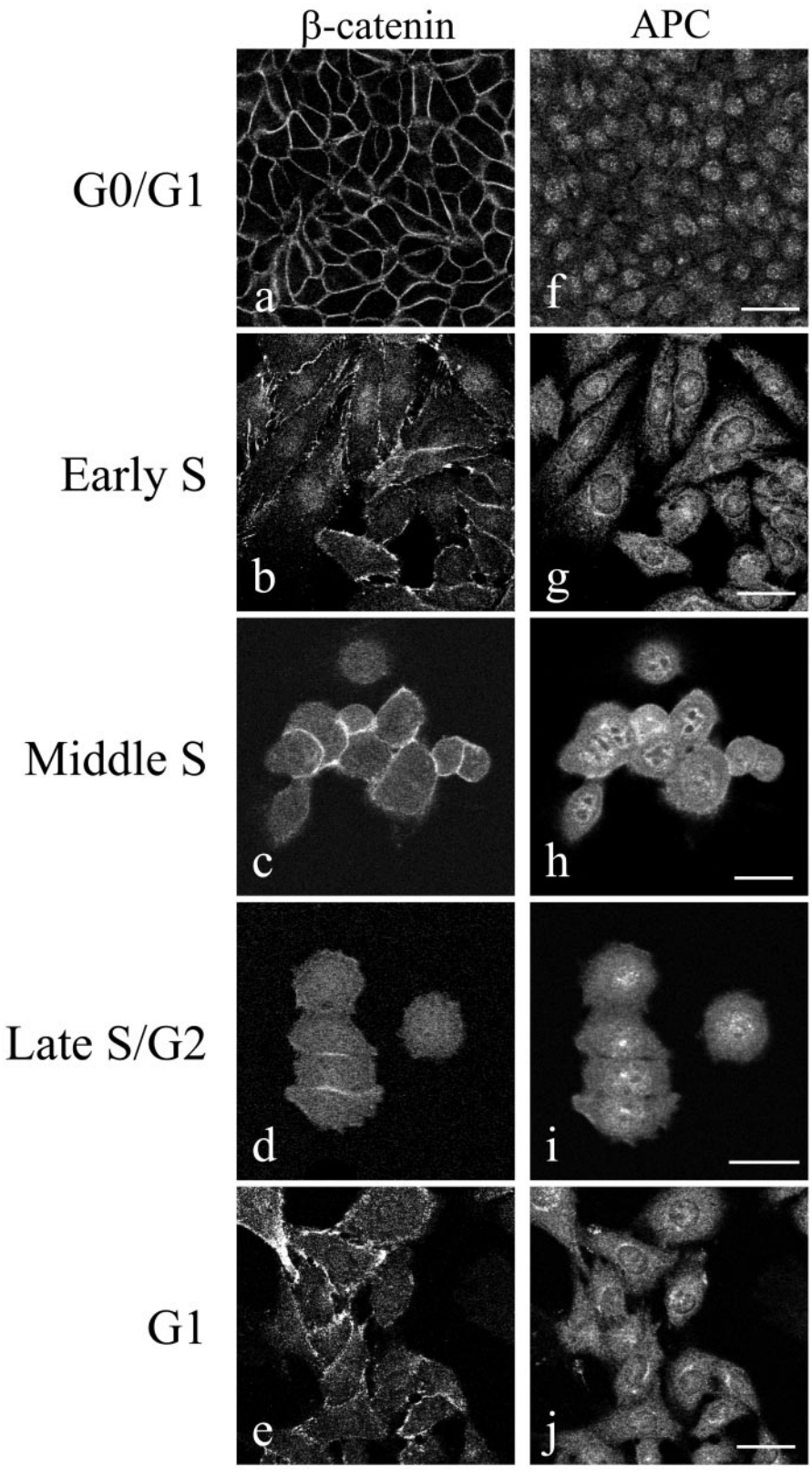

Figure 3. β-catenin and APC accumulate in the cytoplasm and nucleus form early S phase to G2. HaCa4 cells were grown on glass coverslips and synchronized by double thymidine block. After release of the second block, cells were fixed at different time points covering a whole cell cycle with methanol and permeabilized with 0.05% NP-40 in PBS for 5 min. Double immunostaining for β-catenin (a–e) and APC (f–j) was performed. Images show confocal planes taken at the center area of the cells. Bars, 20 μm. The DNA content for each time point was measured by flow cytometry in a parallel experiment to determine the phase of the cell cycle.

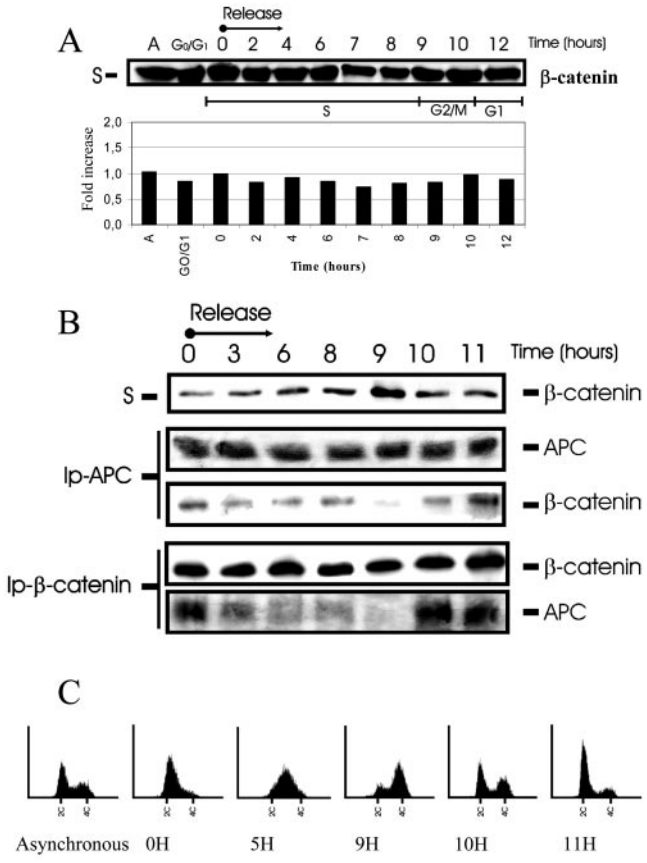

Figure 4. Regulation of β-catenin levels during the cell cycle depends on its interaction with APC. (A) Top panel: Western blot analysis of β-catenin levels in soluble fractions of SW480 cells synchronized at early S phase by double thymidine block (0 h) and at the indicated time points after release of the block. (A) Asynchronous cell populations; G0/G1, synchronized cells by high confluence and serum starvation. Bottom panel: Densitometric analysis. Optic densities were normalized to those detected at time point 0 h. (B) Immunoprecipitation of β-catenin/APC during the cell cycle. Top: Input soluble β-catenin; bottom: coimmunoprecipitation analyses of β-catenin/APC complexes with anti-APC (Ip-APC) and anti–β-catenin (IP-β-catenin) antibodies, followed by Western blot analysis of β-catenin and APC, as indicated. (C) Flow cytometry analysis of synchronized HaCa4 cells used for this experiment. Results were confirmed in two independent experiments.

Changes in Cytoplasmic β-Catenin Levels during the Cell Cycle Involves Alteration of β-Catenin/APC Interaction

The dramatic rise in the soluble β-catenin levels observed during late S/G2 phase of the cell cycle suggested a transient accumulation of β-catenin at this stage and pointed to changes in β-catenin/APC interaction during the cell cycle. Analysis of synchronized SW480 cells, expressing a truncated form of APC containing high levels of cytoplasmic and nuclear β-catenin (Rubinfeld *et al.*, 1997), showed that soluble β-catenin levels remained fairly constant and high in all phases of the cell cycle (Figure 4A), supporting the involvement of APC in the modulation of β-catenin levels during the cell cycle. To further test this hypothesis, double coimmunoprecipitation analysis of APC and β-catenin were performed with the soluble fraction of HaCa4 cells synchronized at early S phase (Figure 4, B and C). An apparent decrease in β-catenin/APC interaction was observed following release of the cells from the thymidine block and during the S-phase. Almost undetectable levels of β-catenin/APC complexes could be detected at G2/M (9 h after release of the block, Figure 4, B and C), corresponding with the maximum levels of soluble β-catenin (Figure 4B; see also Figure 1C). Strong interaction of β-catenin with APC was again detected as the cells started to enter into a new G1 phase (10–11 h after release), coinciding with decreased levels of soluble β-catenin. Similar results were obtained with synchronized MCA3D cells (our unpublished results). Taken together, these data strongly support the participation of β-catenin/APC interaction in the regulation of cytoplasmic β-catenin levels during the cell cycle.

Blockade of β-Catenin Degradation Leads to G2/M Cell Cycle Arrest

The apparent changes in β-catenin levels during the cell cycle, particularly the transient increase at late S to G2/M and the abrupt decrease at the subsequent G1 phase, suggested a role for β-catenin in the control of G2/M transition or early G1. To test the implication of β-catenin regulation in the control of the cell cycle, we firstly analyzed whether the inhibition of endogenous β-catenin downregulation affects cell cycle progression. To this end, MCA3D cells synchronized at early S phase were treated 2 h after release of the second thymidine block with lithium chloride, an inhibitor of GSK-3β activity (Hedgepeth *et al.*, 1997). Flow cytometry analysis showed that control and lithium-treated cells progressed correctly through the cell cycle until the DNA content had been duplicated reaching to G2/M by 8 h (Figure 5A). Thereafter, control cells progressed into the cell cycle, whereas lithium-treated cells became arrested at G2/M, maintaining a 4C DNA content by 16 h (Figure 5A, 16-h panels). A high proportion of lithium-treated cells remained arrested at G2/M up to 24 h, but a fraction of the cells were apparently able to progress into the cell cycle or enter into apoptosis (Figure 5A, 24-h lithium panels), suggesting that some cells may have escaped the G2/M arrest. In fact, time-lapse video recording showed that lithium-treated cells became apparently arrested at G2, before DNA condensation, by 8 h after release of the thymidine block (Figure 5B). Most of the lithium-treated cells started to dye 20 h after release of the block, although some cells divided before dying probably representing the population that escaped the initial G2/M arrest (Figure 5A, video 1). Western blot analysis of soluble β-catenin levels showed the dynamic changes observed in control cells: a five- to sixfold increase at G2/M phase (8 h) followed by a quick decrease of β-catenin after reentering into G1 phase (Figure 5C). Cells treated with lithium showed a steady increase in soluble β-catenin levels up to 10 h (G2/M-arrested cells) when an eightfold increase over the basal level (0 h) was detected and then started to decrease slowly (Figure 5C). Analysis of the PARP antigen in total extracts of S-phase–synchronized cells provided a formal proof for induction of apoptosis in lithium-treated cells. Degradation of PARP started to be detected by 16 h, coinciding with the G2/M arrest, and became evident after

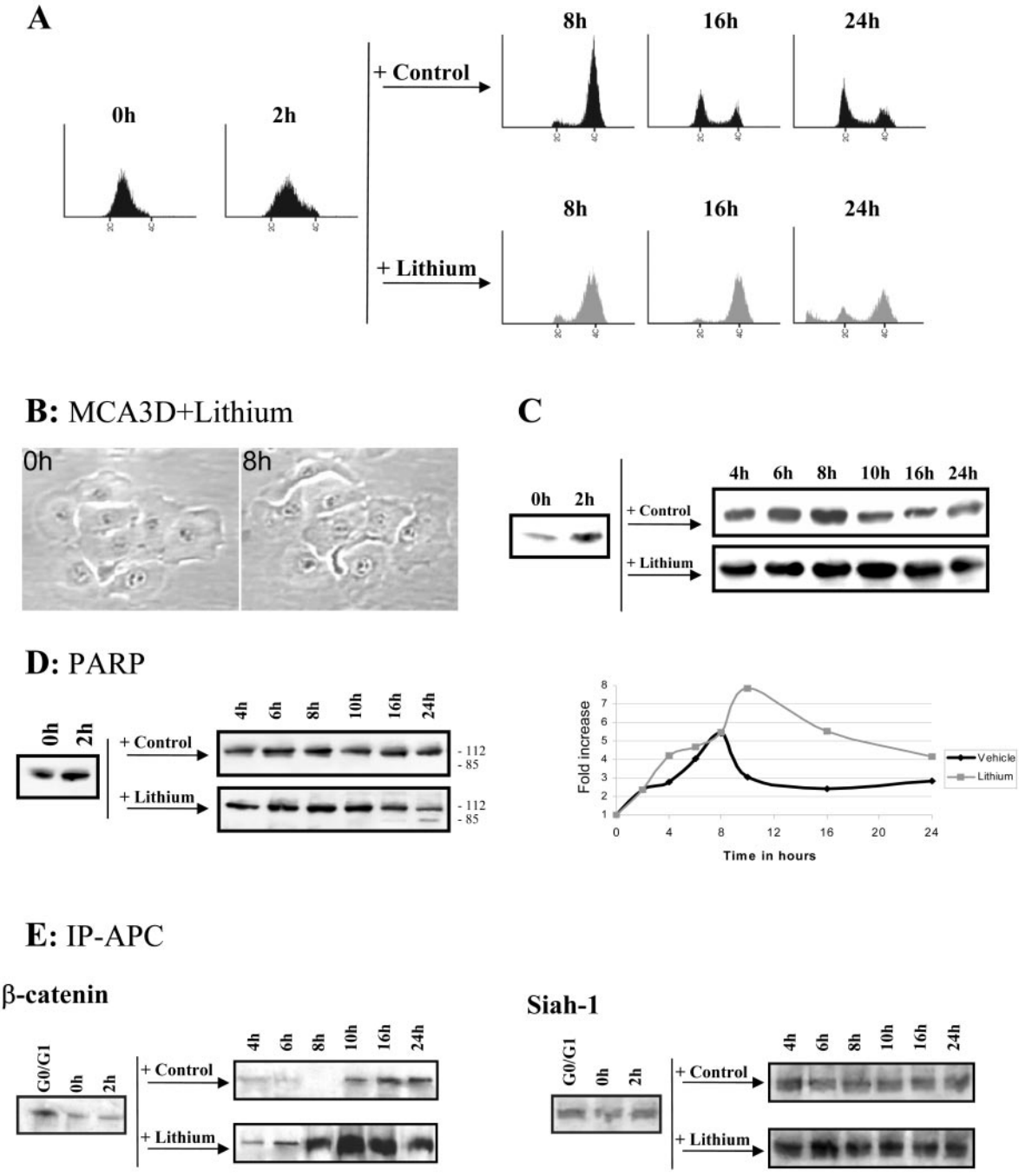

Figure 5. Block of β-catenin degradation leads to β-catenin accumulation, G2/M cell cycle arrest, and induction of apoptosis. MCA3D cells were synchronized by double thymidine block (0 h) and 2 h after release of the block (point 2 h) were treated either with 20 mM NaCl (control) or 20 mM LiCl (lithium) and collected thereafter at the indicated time points. (A) Flow cytometry analysis of synchronized MCA3D cells at early S (0 h), 2 h after release of the block (2 h), and at the indicated time points in control (top panels) or lithium-treated cells (bottom panels). (B) Phase contrast images of S-phase–synchronized MCA3D cells treated with 20 mM LiCl. Still images were taken immediately (0 h) and 8 h after release of the second thymidine block (6 h of lithium treatment). (C) Western blot analysis of β-catenin soluble levels obtained in the same experimental conditions as in A. Densitometric analyses are shown at the bottom; optic densities are referred to those found at time point 0 h. (D) Analysis of PARP antigen degradation. Total protein extracts obtained at the indicated time points for each experimental condition and subjected to Western blot with anti-PARP antibodies. Similar results were obtained in three independent experiments. (E) Analysis of APC/β-catenin and APC/Siah-1 interaction in control and lithium-treated cells. Soluble fractions of MCA3D cells were obtained in the same experimental conditions as in A and were immunoprecipitated with anti-APC antibody followed by Western blot analysis of coimmunoprecipitated β-catenin (left) or Siah-1 (right). The soluble fraction of G0/G1 cells was also included in the immunoprecipitation and Western blot analyses.

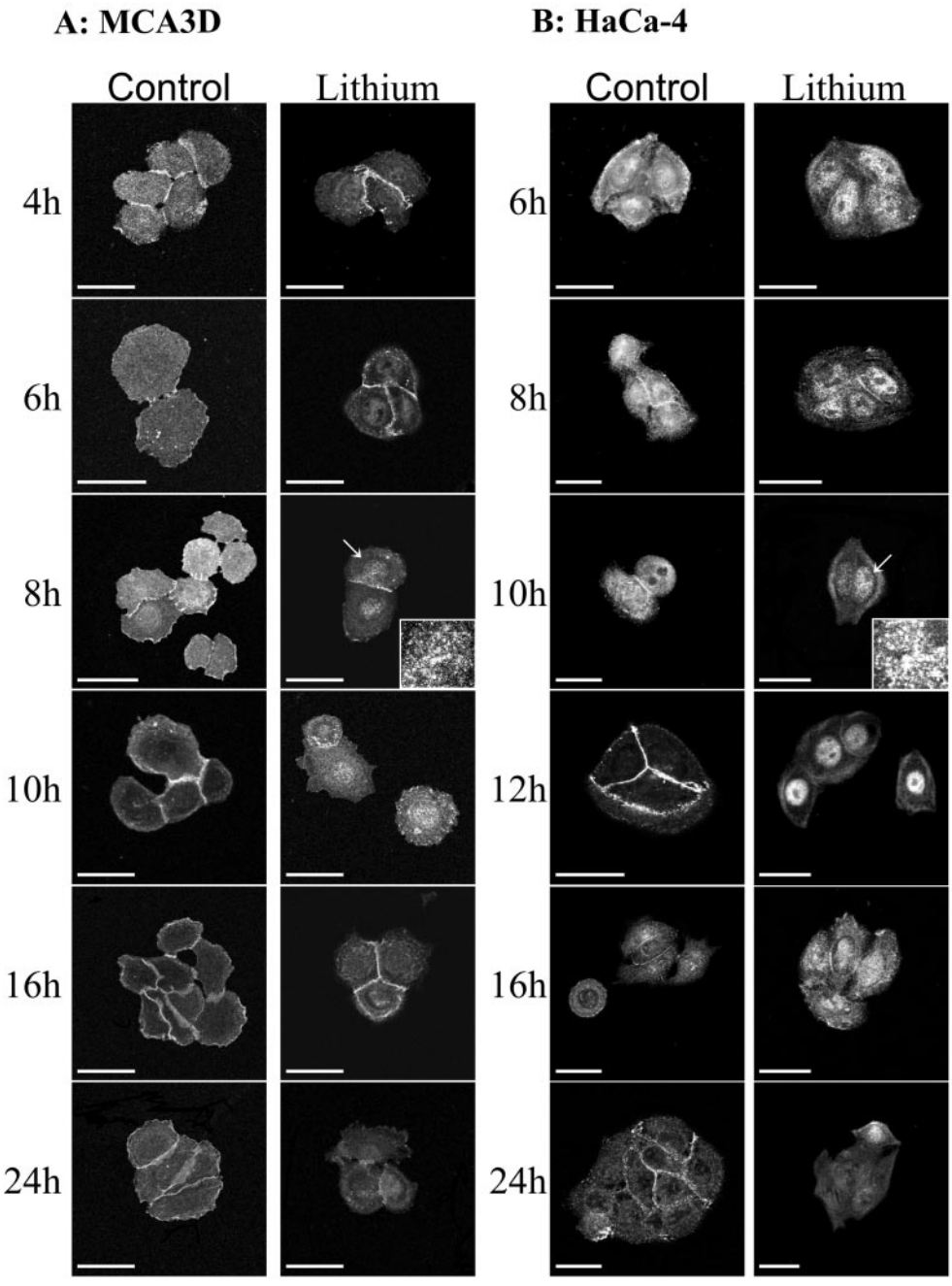

Figure 6. Treatment with lithium chloride in S-phase–synchronized cells induces β-catenin accumulation and its nuclear translocation. MCA3D (A) and HaCa4 cells (B) were grown on glass coverslips and synchronized at early S by double thymidine block and treated as described in Figure 5. Two hours after release of the block, cells were treated with 20 mM LiCl (lithium panels) or 20 mM NaCl (control panels). Cells were fixed at different time points and stained for β-catenin. Confocal images show projections of the central region of the cells. Insets show magnified images, indicated by arrows, of the nuclear region. Bars, 20 μm.

24 h of treatment (Figure 5D, compare control and lithium panels).

The involvement of APC in the G2/M arrest was also investigated. Immunoprecipitation analyses were performed in control and lithium-treated MCA3D cells after S-phase synchronization. APC/β-catenin interaction was observed at all time points of lithium treatment, with a dramatic increase from 8 to 16 h, and remaining fairly high up to 24 h after treatment, in contrast with the dynamics of APC/β-catenin interaction detected in control cells (Figure 5E, left panels; see also Figure 4B). The strong increase in APC/β-catenin association in lithium-treated cells coincided with the G2/M arrest and with the maintained high levels of soluble β-catenin (Figure 5, A and C).

These results indicate that cytoplasmic β-catenin accumulation induced by lithium treatment does not preclude formation of β-catenin/APC complexes that are, nevertheless, unproductive for β-catenin degradation, in agreement with previous results observed with N-terminal–truncated β-catenin forms (Munemitsu *et al.*, 1996). The strong β-catenin/APC interaction observed in lithium-treated cells also suggest that a significant fraction of the

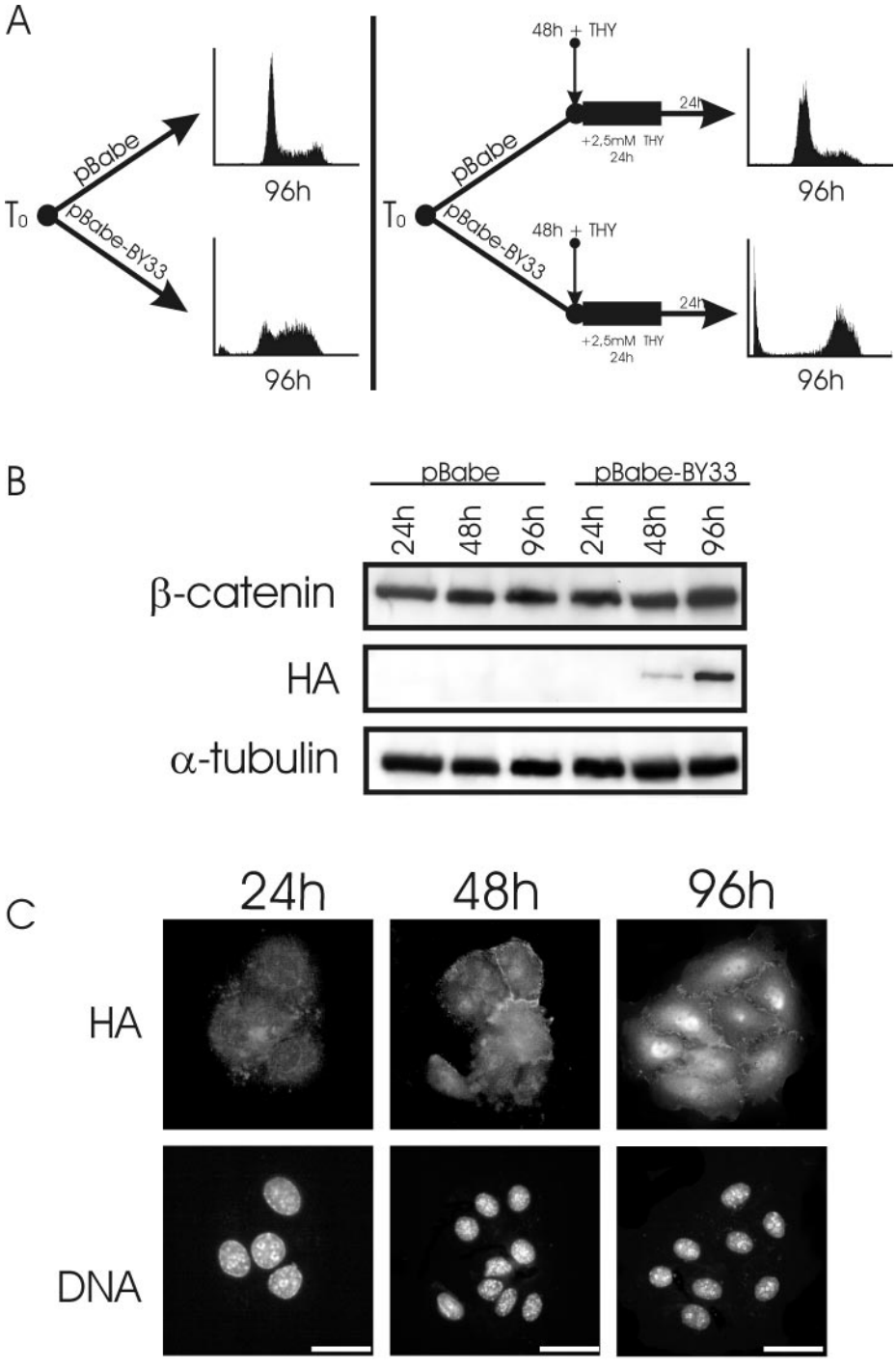

Figure 7. Overexpression of a stable form of β-catenin leads to G2/M arrest and apoptosis. PB cells were infected either with the retroviral construction pBabe-HA-β-catenin(BY33) (pBabe-BY33) or the control construction pBabe. (A) Flow cytometry analyses of PB cells 96 h after infection (left), or after a single thymidine (THY) treatment performed 48 h after infection, and analyzed 24 h after release of the block (right panels). (B) Western blot analysis of β-catenin (total and ectopic) proteins levels in whole cell extracts obtained from PB cells either infected with pBabe construction or pBabe-BY33 at different time points after infection. As a loading control, Western blot analysis of α-tubulin was included. (C) Immunofluorescence analysis of HA-β-catenin (BY33) (top) localization at different time points after infection. DNA was detected by DAPI stain (bottom). Bars, 20 μm.

APC pool might be sequestered in β-catenin complexes in G2/M-arrested cells, although other indirect effects of lithium cannot be presently discarded. Recently, an alternative degradation pathway of β-catenin, independent of GSK-3β and involving APC and Siah-1, has been described (Liu *et al.*, 2001; Matsuzawa and Reed, 2001). Its potential participation in the downregulation of β-catenin at late time points of lithium treatment was then investigated. Siah-1 was detected associated to APC immunoprecipitates at fairly constant levels during the cell cycle in control and lithium-treated cells (Figure 5E, right panels), although increased levels of APC/Siah-1 complexes were observed at all time-points in lithium-treated cells (>2–3-fold over control cells).

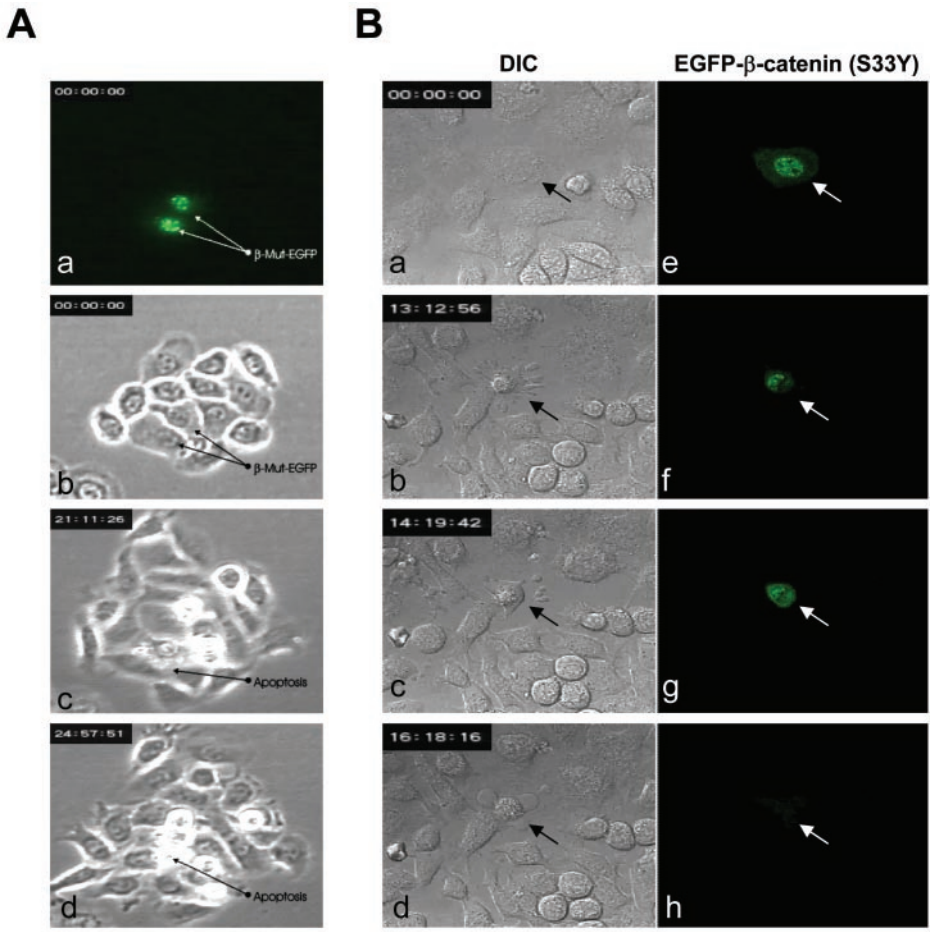

Figure 8. Induction of EGFP-β-catenin leads to apoptosis. MCA3D cells were cotransfected with the pIND-β-catenin(S33Y) and pVgRXR constructions and then S-phase–synchronized by double thymidine block. EGFP-β-catenin(S33Y) expression was induced by adding 1 mM muristerone to the growth medium 6 h before the release of the second thymidine block. (A) Time-lapse video recording in an Axiovert microscope was initiated immediately after release of the block for up to 30 h. (a and b) Still images at time 0.00 showing (a) fluorescence field with two EGFP-β-catenin(S33Y) expressing cells and (b) phase contrast of the same field. (c and d) Still phase contrast images taken at 21 h (c) and 25 h (d) showing apoptosis of the EGFP-β-catenin(S33Y)–expressing cells, indicated by arrows. (B) Confocal time-lapse video recording was initiated 10 h after release of the block for up to 18 h. Still images of the cultures were taken at the indicated time points, showing DIC images (left) or green fluorescent images (right) of the same field. Note that induction of apoptosis in the EGFP-β-catenin(S33Y)–expressing cell (indicated by arrows) coincides with the release of EGFP-β-catenin(S33Y) to the cytosol, followed by complete disappearance of EGFP-β-catenin(S33Y).

To further investigate the significance of increased β-catenin levels at G2/M, we performed parallel analysis of its subcellular localization during the cell cycle in control and lithium-treated MCA3D and HaCa4 cells. A clear accumulation of β-catenin in the nucleus was observed in both cell lines after lithium chloride treatment (Figure 6, A and B, lithium panels), in contrast to control cells, which showed an even stain between cytoplasm and nucleus (Figure 6, control panels; see also Figure 3). Nuclear accumulation of β-catenin in lithium-treated cells started to be detected 6 h after release of the thymidine block, and maximum nuclear fluorescence intensity was detected after 8–10 h (MCA3D) and 10–12 h (HaCa4; Figure 6, A and B). Nuclear β-catenin showed a punctate staining pattern that would be compatible with sites of active transcription at G2/M, in agreement with the recent identification of AF17 as a G2/M β-catenin target gene (Lin *et al.*, 2001). Twenty-four hours after release of the thymidine block, β-catenin started to disappear from the nucleus in lithium-treated cells (Figure 6, A and B, 24-h panels), coinciding with reentering of at least a fraction of cells into a new G1 phase or into apoptosis (Figure 5A, lithium panels, and Figure 5D). Lithium treatment of asynchronous MCA3D and HaCa4 cells also induced G2/M arrest and strong β-catenin nuclear stain, but SW480 cells with mutant APC did not respond to the cell cycle arrest (supplemental Figure 2).

Overexpression of Stable β-Catenin Induces G2/M Arrest

To provide direct evidence that β-catenin stabilization is responsible of the G2/M arrest, the effect of overexpression of a mutant stable β-catenin(S33Y) was analyzed. Repeated attempts to generate stable transfectants in several epidermal keratinocyte cell lines failed, as previously reported in a variety of cell systems (Kim *et al.*, 2000), suggesting a deleterious effect of this mutant β-catenin form. Retroviral transduction in PB keratinocyte cells was then chosen because it has been shown to successfully work in MEFs (Damalas *et al.*, 1999, 2001). Time-course cell cycle analyses were performed from 24 to 96 h after transduction in asynchronous cell populations. No significant changes in the cell cycle distribution were observed after 24 and 48 h (our unpublished results), but after 96 h a clear accumulation of cells at G2/M was detected in the β-catenin(S33Y)–transduced cells, in contrast to the normal distribution of control cells transduced with the pBABE control vector (Figure 7A, left panels). Western blot analysis with anti-HA antibodies of the ectopic mutant β-catenin showed high expression level 96 h

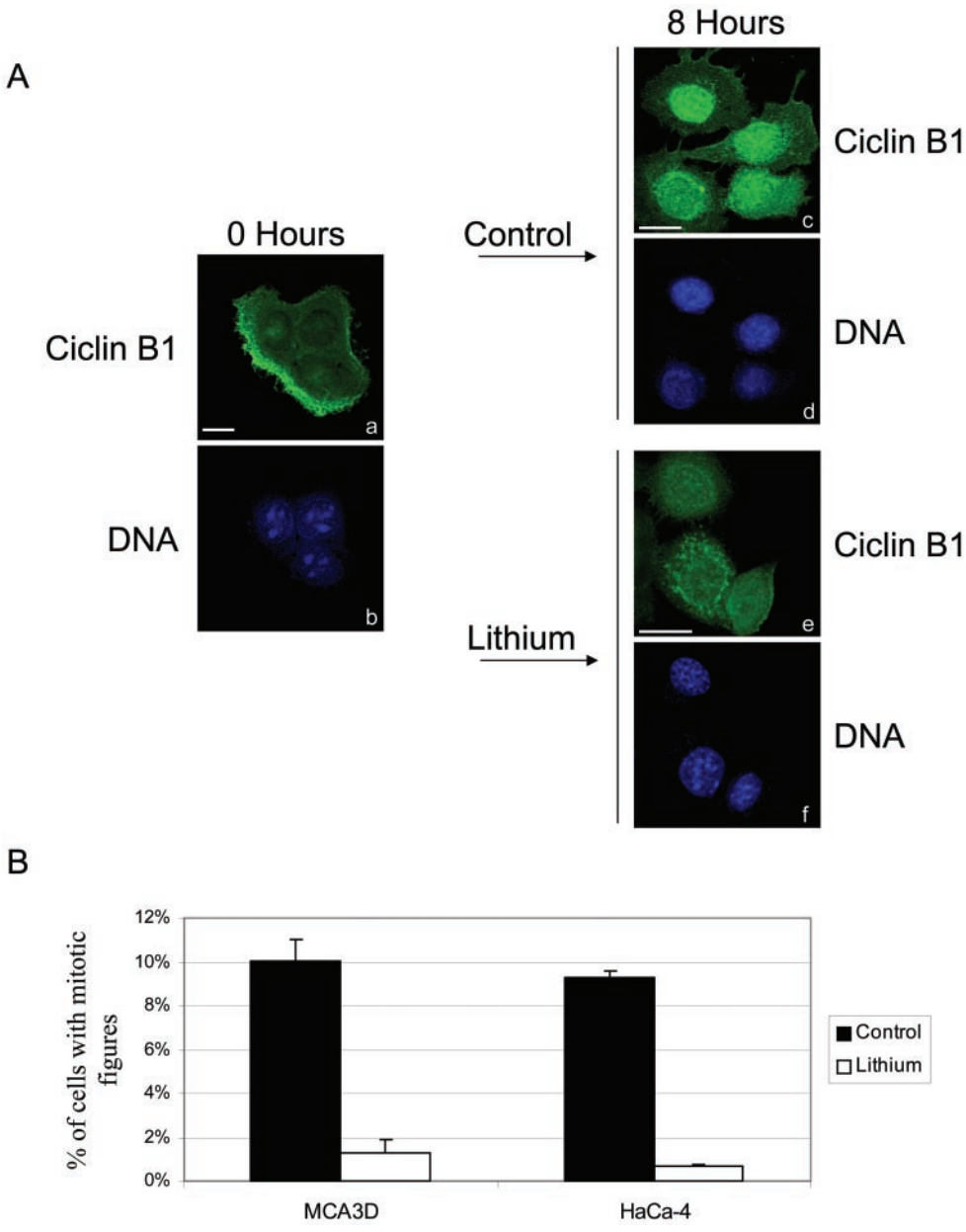

Figure 9. Blockade of β-catenin degradation induces a G2 arrest. (A) MCA3D cells grown on coverslips were synchronized by double thymidine block and 2 h after release treated with 20 mM NaCl (Control) or 20 mM LiCl (Lithium), as indicated in Figure 5. Cells were fixed immediately (0 h; a and b) or at 8 h (c–f) after release of the block and immunostained for cyclin B1 (a, c, and e) and stained for DNA (DAPI stain; b, d, and f). Confocal images show projections of the central region of the cells. Bars, 20 μm. Note the strong and almost exclusive nuclear localization of cyclin B1 in control cells, in contrast to lithium-treated cells, 8 h after release of the block. (B) MCA3D (left) and HaCa4 cells (right) were asynchronously grown on coverslips, treated for 18 h with 20 mM NaCl (Control, ■), or 20 mM LiCl (Lithium, □). Cells were then fixed and stained for DNA with DAPI. The number of mitotic figures was estimated by direct counting on an Axiophot microscope on five independent fields performed on three independent preparations for each experimental condition. The percentage of cells with mitotic figures is represented, as the average ± SD.

after transduction, coinciding with an increase in total β-catenin levels (Figure 7B; 1.5-fold increase after normalization for α-tubulin levels). PB cells transduced with β-catenin(S33Y) showed nuclear stain of mutant β-catenin 96 h after infection, whereas it was mainly present at cell-cell contacts 48 h after transduction (Figure 7C) when no effect on the cell cycle is observed. Control and β-catenin(S33Y)–transduced PB cells were also synchronized by a single thymidine block 48 h after transduction. As shown in Figure 7A (right panels) a clear G2/M arrest was induced 24 h after release of the block in the β-catenin(S33Y)–transduced cells, whereas synchronized control cells normally progressed into the cell cycle. Synchronized β-catenin(S33Y)–transduced cells maintained levels of mutant β-catenin protein similar to those found in asynchronous cell populations 96 h after transduction (Figure 7B; our unpublished results). A fraction of the β-catenin(S33Y)–transduced cells both asynchronously growing for 96 or 24 h after synchronization were detected into the subG1 population, suggesting induction of apoptosis (Figure 7A, lower panels).

To provide additional evidence for a direct effect of β-catenin accumulation in cell cycle and apoptosis, transient transfection of an inducible EGFP-β-catenin(S33Y) form, using the ecdisone-inducible system, was performed in MCA3D cells followed by S-phase synchronization. Expression of mutant EGFP-β-catenin(S33Y) in this system was not efficient enough to perform biochemical assays, but allowed video-lapse studies. This kind of analyses (Figure 8, videos 2

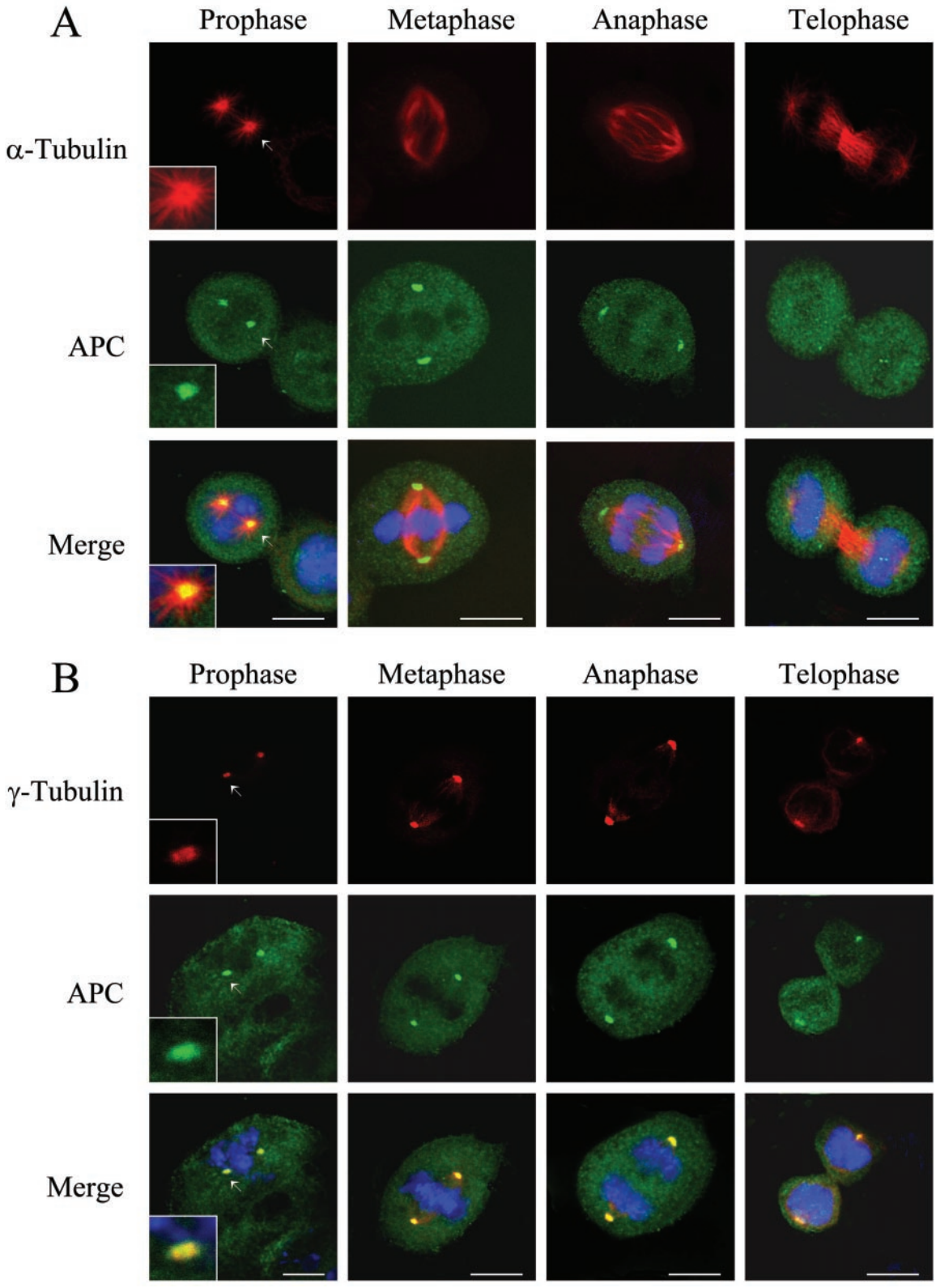
A
Prophase
Metaphase
Anaphase
Telophase
α-Tubulin
APC
Merge
B
Prophase
Metaphase
Anaphase
Telophase
γ-Tubulin
APC
Merge

Figure 10.

and 3) clearly showed that those cells expressing stable EGFP-β-catenin were unable to progress into the cell cycle, being apparently arrested at G2/M, and then were directed to apoptosis without entering into mitosis, in contrast to adjacent nonexpressing cells, which divided normally.

Taken together, these results support a main role for β-catenin in the control of cell cycle and apoptosis at G2/M.

Blockade of β-Catenin Degradation Induces Arrest at G2

The observed G2/M arrest induced by overexpression of β-catenin could affect either entry of the cells into M or, alternatively, their exit from M. To analyze the specific point at G2/M where the arrest was induced, we analyzed the nuclear localization of cyclin B1 in S-phase–synchronized control and lithium-treated MCA3D cells (Figure 9A). Confocal immunofluorescence analysis showed a strong and almost exclusive nuclear localization of cyclin B1 in synchronized control cells 8 h after release of the thymidine block (Figure 9A, c and d). In contrast, lithium-treated cells exhibited a weaker cyclin B1 stain that was mainly detected in the cytoplasm in the majority of cells 8 and 16 h after release of the block (Figure 9A, e and f; our unpublished results), supporting that they were arrested at G2. To further confirm the G2 arrest, the number of mitotic figures present in asynchronally growing control and lithium-treated MCA3D and HaCa4 cells was determined. As shown in Figure 9B, almost a complete absence of mitotic figures was detected in lithium-treated cells after 18 h of treatment, coinciding with the G2/M arrest, whereas ~10% of control cells were at mitosis. These data, together with the video-lapse analyses of lithium-treated cells and β-catenin(S33Y)–overexpressing cells (Figures 5B and 8), showing that cells were apparently arrested before DNA condensation, strongly support that β-catenin accumulation induces a G2 arrest, thus precluding entering of cells into mitosis.

APC Accumulates at Centrosomes from Late S to the End of M Phase

The apparent localization of APC at centrosomes at late S/G2 suggested by our results (see Figure 3) and by previous reports (Tighe *et al.*, 2001), led to a detailed confocal microscopy analysis of the APC distribution during different stages of M phase of the cell cycle (Figure 10). Double immunofluorescence analysis of APC and α-tubulin showed the colocalization of both molecules at centrosomes from prophase to anaphase, apparently associated to the microtubule organizing center (MTOC; Figure 10A). Recent studies have implicated APC in the binding of microtubules to the kinetochores at the mitotic spindle (Fodde *et al.*, 2001; Kaplan *et al.*, 2001). The presence of APC at the kinetochores could not be confirmed in our analyses, probably because of the lower resolution of our images that precluded the analysis of those small structures. Analysis of confocal images shown in Figure 10A indicated that APC accumulates at the center of the MTOC from where microtubules irradiate to form the mitotic spindle at prophase (Figure 10A, prophase, inset). This observation supported the presence of APC at the pericentriolar matrix.

To further analyze this fact, double immunofluorescence analysis with the γ-tubulin centrosome marker was performed. A strong colocalization between APC and γ-tubulin was observed during mitosis (Figure 10B). Colocalization between both molecules could be detected from middle-late S phase (our unpublished results), but strong accumulation of APC at the pericentriolar matrix was observed once the centrioles have duplicated and colocalized with γ-tubulin (Figure 10B, prophase, inset). APC remained at these structures throughout M phase always in apparent association with the mitotic poles. Similar analysis carried out in the SW480 cell line also showed the colocalization of APC with the MTOC (our unpublished results). Analysis of β-catenin distribution in M phase showed a diffuse staining and absence of localization at the centrosomes (supplemental Figure 3). In contrast to these observations, the association of APC to centrosomes was significantly decreased in lithium-treated cells (our unpublished results), supporting that the strong APC/β-catenin interaction detected in those cells (see Figure 5E) might preclude its interaction with other cellular structures, such as the centrosomes.

Figure 10 (facing page). APC localizes to centrosomes at the MTOC during the M phase. HaCa4 cells grown on glass coverslips were synchronized by double thymidine block and allowed to progress through the cell cycle until they reached M phase, when they were fixed. (A) HaCa4 cells stained for α-tubulin (top panels, red), APC (middle panels, green), and DNA (bottom panels, TO-TO-3, blue). Merge images are shown in the lower panels. Insets: Magnified images, indicated by arrows, showing APC colocalization with the (−) ends of the microtubules at prophase. (B) HaCa4 cells stained for γ-tubulin (top panels, red), APC (middle panels, green), and DNA (bottom panels, TOTO-3, blue). Merge images are shown in the bottom panels. Insets: magnified images, indicated by arrows, showing APC colocalization with γ-tubulin. Confocal images showed projections of the central region of the cells. Bars, 10 μm.

DISCUSSION

Involvement of β-Catenin in the Control of G2/M and Apoptosis

The involvement of β-catenin signaling in the control of cell cycle is not yet fully understood. Some studies support a positive role in the control of G1/S (Orford *et al.*, 1999), whereas others suggest a potential involvement in cell cycle arrest through the induction of p53 and p19ARF pathway (Damalas *et al.*, 1999, 2001) or a direct involvement in apoptosis (Kim *et al.*, 2000). We have further analyzed this important issue, and in the present report we provide evidence for a direct involvement of β-catenin in the control of cell cycle progression at G2/M in epithelial cell lines of epidermal origin. Analysis of β-catenin levels during the cell cycle from S-phase–synchronized cells showed a steady increase in soluble β-catenin, nonassociated to E-cadherin complexes, and nuclear β-catenin during the S phase with maximum accumulation at G2/M, followed by an abrupt decrease once the cells enter into a new G1 phase. In agreement with these observations, confocal microscopy analysis of β-catenin during the cell cycle showed strongly increased cytoplasmic and nuclear localization during S and G2/M, with a homogenous distribution between both cell compartments. The dramatic increase in β-catenin levels at G2/M, accounting for 5- to 10-fold over basal levels at early S phase, rule out that they are a consequence of junctional reorganization during mitosis and point to a strict regulation of β-catenin levels during the cell cycle. In fact, biochemical

analysis of β-catenin/APC interaction showed dramatic changes in the association of both proteins during the cell cycle in a complementary pattern to β-catenin levels, strongly supporting a direct involvement of APC in the regulation of β-catenin levels during the cell cycle.

All those observations suggested a role for soluble β-catenin in the control of G2/M to G1 transition of the cell cycle. Support for this hypothesis has been obtained from the studies carried out in epidermal keratinocyte cell lines under conditions, which interfere with the destabilization of cytoplasmic β-catenin by 1) overexpression of a mutant stable form of β-catenin(S33Y) and 2) blockade of endogenous β-catenin degradation after S-phase synchronization by lithium treatment. In either experimental situation, cells become cell cycle arrested at G2/M and are further induced to apoptosis. Furthermore, the pattern of cyclin B1 stain, together with the absence of mitotic figures in lithium-treated cells and the video-recording analyses, indicates that β-catenin accumulation induces a G2-arrest. These results are in agreement with previous reports showing induction of apoptosis independent of G1/S regulators by overexpression of stable β-catenin in a variety of cell lines (Kim *et al.*, 2000) and with the proposed role of armadillo signaling in induction of apoptosis and G2/M arrest in *Drosophila* retinal and wing development (Ahmed *et al.*, 1998; Johnston and Edgar, 1998). They also agree with previous studies in bovine aortic endothelial cells in which inhibition of GSK-3β activity by lithium chloride induced a G2/M arrest linked to stabilization of p53 levels (Mao *et al.*, 2001) and with the reported p53 induction by stabilized mutant β-catenin in MEFs (Damalas *et al.*, 1999, 2001). In this regard, our initial studies have also shown a strong accumulation of p53 protein levels in epidermal MCA3D and PB cells in response to increased accumulation of cytoplasmic β-catenin (our unpublished results), suggesting the potential participation of p53 in the β-catenin-induced G2 arrest.

The present results seem to be in apparent contradiction with different reports supporting that activating mutations of β-catenin in different tumors confer a proliferative advantage (Polakis, 1999) and with reports in other cell systems and transgenic mice in which stable β-catenin mutants also lead to increased proliferation. Several considerations can be made in relation to those previous data.

1. Many studies of overexpression of mutant β-catenin have been performed with N-terminal–truncated versions (see for instance, Barth *et al.*, 1997; Munemitsu *et al.*, 1996; Gat *et al.*, 1998), which indeed result in stable nondegradable β-catenin. However, the N-terminal region of β-catenin contains a transactivation domain (Aoki *et al.*, 2002) whose deletion can potentially influence the expression of target genes in those models. Furthermore, in different transgenic models using ΔN-β-catenin distinct phenotypes are observed, ranging from induction of proliferation only in restricted areas of epidermis (Gat *et al.*, 1998) to induction of proliferation, differentiation, and/or apoptosis in different epithelial tissues (Wong *et al.*, 1998; Imbert *et al.*, 2001; Gounari *et al.*, 2002).

2. Several studies have shown that overexpression of normal or stable β-catenin with point mutations in the phosphorylable residues in different cell systems either does not induce increased proliferation (Young *et al.*, 1998), interferes with cell survival (Kim *et al.*, 2000; this work), or induces senescence (Damalas *et al.*, 2001).

3. In some developmental context and cell systems, β-catenin signaling in fact induces G2/M arrest or apoptosis (Ahmed *et al.*, 1998; Johnston and Edgar, 1998; Mao *et al.*, 2001).

4. Cell lines carrying truncated versions of APC and inactivated p53, such as SW480 carcinoma cells (Sharma *et al.*, 1993; Rubinfeld *et al.*, 1997), seem to escape regulation of β-catenin levels during the cell cycle (Figure 4A) and are insensitive to G2/M arrest induced by lithium treatment.

All these observations support that the cell or tissue context might be determinant for the regulation and biological effects of β-catenin during the cell cycle. Furthermore, they suggest that the oncogenic potential of β-catenin can be modulated by the genetic context, additional acquired mutations, particularly those affecting the p53 and/or H-Ras status (Damalas *et al.*, 1999, 2001), and/or by growth factor signals (Muller *et al.*, 2002). Our present results support that in cell lines with normal APC and p53 products, such as epidermal keratinocytes analyzed here, a tight regulation of cytoplasmic β-catenin (nonassociated to adhesion complexes) during G2 to M transition is required to allow the correct progression of cells into the cell cycle.

A New Role for APC in the Organization of the MTOC

The subcellular localization of APC in synchronized MCA3D and HaCa4 cells changes dynamically during the cell cycle, with a clear nuclear accumulation from middle S to G2 (see Figure 3). These results differ from those recently reported in MDCK cells, showing that nuclear accumulation of APC mainly depends on cell density (Zhang *et al.*, 2001) and could be explained by differences in the experimental conditions or the cell systems. Our present results also show that APC is associated to the centrosomes from late S to M phases in MCA3D and HaCa4 cells, colocalizing with γ-tubulin at the MTOC during mitosis (Figure 10). The association of mutant APC to the centrosomes and MTOC has also been detected in SW480 synchronized cells (our unpublished results) and in interphase (Tighe *et al.*, 2001). Localization of *Drosophila* APC2 and APC1 with the centrosomes has also been reported in early embryos and embryonic epidermal and neuroblast cells (McCartney *et al.*, 1999; Akong *et al.*, 2002a, 2002b). These observations indicate that localization of APC to the centrosomes and MTOC is independent of its C-terminal domain and support an additional role for APC in the organization and/or function of the mitotic spindle, distinct from its association to the kinetochores (Fodde *et al.*, 2001; Kaplan *et al.*, 2001).

In contrast with the defined localization of APC from middle S to M, no specific localization of β-catenin at any particular nuclear or subcellular structures could be detected during the cell cycle, apart from the cell membrane. Indeed, no apparent colocalization of β-catenin with APC could be detected from late S to M phase. These results, together with the apparent lack of β-catenin/APC interaction detected at G2/M in control cells, suggest a differential role for both molecules at these specific stages of the cell cycle. In this context, it is tempting to speculate that interaction of APC with microtubule-binding proteins and further association to the centrosomes and/or kinetochores

during late S to G2/M can compete with β-catenin interaction, thus favoring stabilization of cytoplasmic β-catenin at late S/G2 phases observed here. Increased stabilization of β-catenin at late S/G2 could potentially result in direct or indirect activated expression, or accumulation, of genes required for the control of G2/M transition, such as p53 and AF17 (Damalas *et al.,* 1999; Lin *et al.,* 2001; Chan and Struhl, 2002) or in induction of apoptotic or senescence programs under maintained β-catenin levels (Damalas *et al.,* 2001; this work). On the other hand, the strong association of β-catenin with APC observed in G2-arrested cells might support that maintenance of unproductive β-catenin/APC complexes can compete with other APC interactions required for further progression of the cell cycle.

In summary, the results reported here indicate that β-catenin levels are dynamically regulated during the cell cycle and support a direct role for β-catenin in the control of G2/M transition and apoptosis in epidermal keratinocytes. Our results also provide evidence for the implication of APC in the control and/or organization of the MTOC.

ACKNOWLEDGMENTS

We thank C. Calés and N. Vilaboa for advice in the synchronization assays and reagents, L. Rico and F. Larcher for help with retrovirus production, D. Megías for helpful assistance with confocal microscopy, and M.C. Iglesias for reading the manuscript. This work was supported by grants from the Comisión Interministerial de Ciencia y Tecnología (SAF98–0085-C03–01 and SAF2001–2819), Instituto de Salud Carlos III (FIS01/1174) and Comunidad Autónoma de Madrid (08.1/0055/2000) to AC. During the realization of this work D.O. was a predoctoral fellow of the Spanish Ministry of Science and Technology.

REFERENCES

Aberle, H., Schwartz, H., and Kemler, R. (1996). Cadherin-catenin complex: protein interactions and their implications for cadherin function. J. Cell Biochem. *61,* 514–523.

Ahmed, Y., Hayashi, S., Levine, A., and Wieschaus, E. (1998). Regulation of armadillo by a Drosophila APC inhibits neuronal apoptosis during retinal development. Cell *93,* 1171–1182.

Akong, K., Grevengoed, E., Price, M., McCartney, B., Hayden, M., DeNofrio, J., and Peifer, M. (2002a). Drosophila APC2 and APC1 play overlapping roles in Wingless signaling in the embryo and imaginal discs. Dev. Biol. *250,* 91–100.

Akong, K., McCartney, B., and Peifer, M. (2002b). Drosophila APC2 and APC1 have overlapping roles in the larval brain despite their distinct intracellular localizations. Dev. Biol. *250,* 71–90.

Aoki, M., Sobek, V., Maslyar, D.J., Hecht, A., and Vogt, P.K. (2002). Oncogenic transformation by β-catenin: deletion analysis and characterization of selected target genes. Oncogene *21,* 6983–6991.

Barth, A.I., Pollack, A.L., Altschuler, Y., Mostov, K.E., and Nelson, W.J. (1997). NH2-terminal deletion of β-catenin results in stable colocalization of mutant β-catenin with adenomatous polyposis coli protein and altered MDCK cell adhesion. J. Cell Biol. *136,* 693–706.

Behrens, J., Jerchow, B.A., Wurtele, M., Grimm, J., Asbrand, C., Wirtz, R., Kuhl, M., Wedlich, D., and Birchmeier, W. (1998). Functional interaction of an axin homolog, conductin, with β-catenin, APC, and GSK3β. Science *280,* 596–599.

Bienz, M. (2002). The subcellular destinations of apc proteins. Nat. Rev. Mol. Cell. Biol. *3,* 328–338.

Chan, S.K., and Struhl, G. (2002). Evidence that armadillo transduces Wingless by mediating nuclear export or cytosolic activation of pangolin. Cell *111,* 265–280.

Cui, H., Dong, M., Sadhu, D., and Rosenberg, D. (2002). Suppression of kinesin expression disrupts adenomatous polyposis coli (APC) localization and affects β-catenin turnover in young adult mouse colon (YAMC) epithelial cells. Exp. Cell Res. *280,* 12–23.

Damalas, A., Ben-Ze'ev, A., Simcha, I., Shtutman, M., Leal, J.F., Zhurinsky, J., Geiger, B., and Oren, M. (1999). Excess β-catenin promotes accumulation of transcriptionally active p53. EMBO J. *18,* 3054–3063.

Damalas, A., Kahan, S., Shtutman, M., Ben-Ze'ev, A., and Oren, M. (2001). Deregulated β-catenin induces a p53- and ARF-dependent growth arrest and cooperates with Ras in transformation. EMBO J. *20,* 4912–4922.

Espada, J., Pérez-Moreno, M.A., Braga, V.M., Rodriguez-Viciana, P., and Cano, A. (1999). H-Ras activation promotes cytoplasmic accumulation and phosphoinositide 3-OH kinase association of β-catenin in epidermal keratinocytes. J. Cell Biol. *146,* 967–980.

Fodde, R., *et al.* (2001). Mutations in the APC tumour suppressor gene cause chromosomal instability. Nat. Cell Biol. *3,* 433–438.

Gat, U., DasGupta, R., Degenstein, L., and Fuchs, E. (1998). De novo hair follicle morphogenesis and hair tumors in mice expressing a truncated β-catenin in skin. Cell *95,* 605–614.

Gounari, F. *et al.* (2002). Stabilization of β-catenin induces lesions reminiscent of prostatic intraepithelial neoplasia, but terminal squamous transdifferentiation of other secretory epithelia. Oncogene *21,* 4099–4107.

Gumbiner, B.M. (1995). Signal transduction of β-catenin. Curr. Opin. Cell Biol. *7,* 634–640.

He, T.C., Sparks, A.B., Rago, C., Hermeking, H., Zawel, L., da Costa, L.T., Morin, P.J., Vogelstein, B., and Kinzler, K.W. (1998). Identification of c-MYC as a target of the APC pathway. Science *281,* 1509–1512.

He, T.C., Chan, T.A., Vogelstein, B., and Kinzler, K.W. (1999). PPARdelta is an APC-regulated target of nonsteroidal anti-inflammatory drugs. Cell *99,* 335–345.

Hedgepeth, C.M., Conrad, L.J., Zhang, J., Huang, H.C., Lee, V.M., and Klein, P.S. (1997). Activation of the Wnt signaling pathway: a molecular mechanism for lithium action. Dev. Biol. *185,* 82–91.

Imbert, A., Eelkema, R., Jordan, S., Feiner, H., and Cowin, P. (2001). Delta N89 β-catenin induces precocious development, differentiation, and neoplasia in mammary gland. J. Cell Biol. *153,* 555–568.

Johnston, L.A., and Edgar, B.A. (1998). Wingless and Notch regulate cell-cycle arrest in the developing Drosophila wing. Nature *394,* 82–84.

Kaplan, K.B., Burds, A.A., Swedlow, J.R., Bekir, S.S., Sorger, P.K., and Nathke, I.S. (2001). A role for the Adenomatous Polyposis Coli protein in chromosome segregation. Nat. Cell Biol. *3,* 429–432.

Kim, K., Pang, K.M., Evans, M., and Hay, E.D. (2000). Overexpression of β-catenin induces apoptosis independent of its transactivation function with LEF-1 or the involvement of major G1 cell cycle regulators. Mol. Biol. Cell *11,* 3509–3523.

Korinek, V., Barker, N., Morin, P.J., van Wichen, D., de Weger, R., Kinzler, K.W., Vogelstein, B., and Clevers, H. (1997). Constitutive transcriptional activation by a β-catenin-Tcf complex in APC-/- colon carcinoma. Science *275,* 1784–1787.

Lin, Y.M. *et al.* (2001). Identification of AF17 as a downstream gene of the β-catenin/T-cell factor pathway and its involvement in colorectal carcinogenesis. Cancer Res. *61,* 6345–6349.

Liu, C., Kato, Y., Zhang, Z., Do, V.M., Yankner, B.A., and He, X. (1999). β-Trcp couples β-catenin phosphorylation-degradation and regulates Xenopus axis formation. Proc. Natl. Acad. Sci. USA *96,* 6273–6278.

Liu, J., Stevens, J., Rote, C.A., Yost, H.J., Hu, Y., Neufeld, K.L., White, R.L., and Matsunami, N. (2001). Siah-1 mediates a novel β-catenin degradation pathway linking p53 to the adenomatous polyposis coli protein. Mol. Cell *7,* 927–936.

Lozano, E., and Cano, A. (1998). Cadherin/catenin complexes in murine epidermal keratinocytes: E-cadherin complexes containing either β-catenin or plakoglobin contribute to stable cell-cell contacts. Cell Adhes. Commun. *6,* 51–67.

McCartney, B.M., Dierick, H.A., Kirkpatrick, C., Moline, M.M., Baas, A., Peifer, M., and Bejsovec, A. (1999). Drosophila APC2 is a cytoskeletally-associated protein that regulates wingless signaling in the embryonic epidermis. J. Cell Biol. *146,* 1303–1318.

Mao, C.D., Hoang, P., and DiCorleto, P.E. (2001). Lithium inhibits cell cycle progression and induces stabilization of p53 in bovine aortic endothelial cells. J. Biol. Chem. *276,* 26180–26188.

Matsuzawa, S.I., and Reed, J.C. (2001). Siah-1, SIP, and Ebi collaborate in a novel pathway for β-catenin degradation linked to p53 responses. Mol. Cell *7,* 915–926.

Morin, P.J., Sparks, A.B., Korinek, V., Barker, N., Clevers, H., Vogelstein, B., and Kinzler, K.W. (1997). Activation of β-catenin-Tcf signaling in colon cancer by mutations in β-catenin or APC. Science *275,* 1787–1790.

Muller, T., Bain, G., Wang, X., and Papkoff, J. (2002). Regulation of epithelial cell migration and tumor formation by β-catenin signaling. Exp. Cell Res. *280,* 119–133.

Munemitsu, S., Albert, I., Souza, B., Rubinfeld, B., and Polakis, P. (1995). Regulation of intracellular β-catenin levels by the adenomatous polyposis coli (APC) tumor-suppressor protein. Proc. Natl. Acad. Sci. USA *92,* 3046–3050.

Munemitsu, S., Albert, I., Rubinfeld, B., and Polakis, P. (1996). Deletion of an amino-terminal sequence stabilizes β-catenin in vivo and promotes hyperphosporylation of the adenomatous polyposis coli tumor suppressor protein. Mol. Cell. Biol. *16,* 4088–4094.

Nakamura, M., Zhou, X.Z., and Lu, K.P. (2001). Critical role for the EB1 and APC interaction in the regulation of microtubule polymerization. Curr. Biol. *11,* 1062–1067.

Nathke, I.S., Adams, C.L., Polakis, P., Sellin, J.H., and Nelson, W.J. (1996). The adenomatous polyposis coli tumor suppressor protein localizes to plasma membrane sites involved in active cell migration. J. Cell Biol. *134,* 165–179.

Navarro, P., Gomez, M., Pizarro, A., Gamallo, C., Quintanilla, M., and Cano, A. (1991). A role for the E-cadherin cell-cell adhesion molecule during tumor progression of mouse epidermal carcinogenesis. J. Cell Biol. *115,* 517–533.

Orford, K., Orford, C.C., and Byers, S.W. (1999). Exogenous expression of β-catenin regulates contact inhibition, anchorage-independent growth, anoikis, and radiation-induced cell cycle arrest. J. Cell Biol. *146,* 855–868.

Peifer, M. (1997). β-catenin as oncogene: the smoking gun. Science *275,* 1752–1753.

Polakis, P. (1999). The oncogenic activation of β-catenin. Curr. Opin. Genet. Dev. *9,* 15–21.

Reinacher-Schick, A., and Gumbiner, B.M. (2001). Apical membrane localization of the adenomatous polyposis coli tumor suppressor protein and subcellular distribution of the β-catenin destruction complex in polarized epithelial cells. J. Cell Biol. *152,* 491–502.

Rubinfeld, B., Souza, B., Albert, I., Muller, O., Chamberlain, S.H., Masiarz, F.R., Munemitsu, S., and Polakis, P. (1993). Association of the APC gene product with β-catenin. Science *262,* 1731–1744.

Rubinfeld, B., Albert, I., Porfiri, E., Fiol, C., Munemitsu, S., and Polakis, P. (1996). Binding of GSK3β to the APC-β-catenin complex and regulation of complex assembly. Science *272,* 1023–1026.

Rubinfeld, B., Albert, I., Porfiri, E., Munemitsu, S., and Polakis, P. (1997). Loss of β-catenin regulation by the APC tumor suppressor protein correlates with loss of structure due to common somatic mutations of the gene. Cancer Res. *57,* 4624–4630.

Sharma, S., Schwarte-Waldhoff, I. Oberhuber, H., and Schafer, R. (1993). Functional interaction of wild-type and mutant p53 transfected into human tumor cell lines carrying activated ras genes. Cell Growth Differ. *4,* 861–869.

Shtutman, M., Zhurinsky, J., Simcha, I., Albanese, C., D'Amico, M., Pestell, R., and Ben-Ze'ev, A. (1999). The cyclin D1 gene is a target of the β-catenin/LEF-1 pathway. Proc. Natl. Acad. Sci. USA *96,* 5522–5527.

Tetsu, O., and McCormick, F. (1999). β-catenin regulates expression of cyclin D1 in colon carcinoma cells. Nature *398,* 422–426.

Tighe, A., Johnson, V.L., Albertella, M., and Taylor, S.S. (2001). Aneuploid colon cancer cells have a robust spindle checkpoint. EMBO Rep. *2,* 609–614.

Willert, K., and Nusse, R. (1998). β-catenin: a key mediator of Wnt signaling. Curr. Opin. Genet. Dev. *8,* 95–102.

Wong, M.H., Rubinfeld, B., and Gordon, J.L. (1998). Effects of forced expression of an NH2-terminal truncated β-catenin on mouse intestinal epithelial homeostasis. J. Cell Biol. *141,* 765–777.

Young, C.S., Kitamura, M., Hardy, S., and Kitajewski, J. (1998). Wnt-1 induces growth, cytosolic β-catenin, and Tcf/Lef transcriptional activation in Rat-1 fibroblasts. Mol. Cell. Biol. *18,* 2474–2485.

Yuspa, S.H., Morgan, D., Lichti, U., Spangler, E.F., Michael, D., Kilkenny, A., and Hennings, H. (1986). Cultivation and characterization of cells derived from mouse skin papillomas induced by an initiation-promotion protocol. Carcinogenesis *7,* 949–958.

Zhang, F., White, R.L., and Neufeld, K.L. (2001). Cell density and phosphorylation control the subcellular localization of adenomatous polyposis coli protein. Mol. Cell. Biol. *21,* 8143–8156.